Selected papers presented at the 15th Symposium of Magnetic Measurements and Modelling SMMM'2025

Experimental Investigation of Magnetic Permeability Degradation Due to Welding in 80NI–Fe and 50NI–Fe Magnetic Shielding Alloys

S. Zurek[a,*], G. Voulazeris[b] and P. Marsden[b]

[a] *Megger Instruments Ltd., Archcliffe Road, Dover, Kent, CT17 9EN, United Kingdom*
[b] *Magnetic Shields Ltd., Headcorn Road, Staplehurst, Kent, TN12 0DS, United Kingdom*

Doi: 10.12693/APhysPolA.149.S102 *e-mail: stan.zurek@megger.com

This experimental study investigates welding operation on two magnetic shielding materials (80Ni–Fe and 50Ni–Fe), and the results indicate that, especially at lower excitation amplitude and frequency (50 Hz), the permeability of the welded joints can be significantly lower, i.e., reduced by up to 80% from the original value. At a higher frequency (400 Hz), the apparent degradation is not as severe, mostly because the apparent permeability is significantly lower due to global eddy currents. If welds constitute only a small proportion of the overall volume of the shield, the equivalent permeability is affected proportionally to the reluctance of each part. Recommended annealing is unable to fully recover the initial permeability measured at lower frequencies, but it is beneficial in improving the permeability.

topics: permeability, welding, Mumetal, Ni–Fe alloys

1. Introduction

Magnetic shielding provides critical functionality in many scientific and industrial applications. At direct current (DC) and power frequencies (e.g., up to 400 Hz), shielding is often relied upon by redirecting the path of magnetic flux away from, or around, the shielded object by using an appropriately shaped magnetic circuit. The magnetic reluctance of each part of such a magnetic circuit should be as low as possible in the considered magnetic path. For shielding of low-amplitude magnetic fields, materials with high initial magnetic permeability are used. For some geometries, these materials must also provide the mechanical means for metal forming, so tape-based or ribbon-based high-permeability materials, such as nanocrystalline ones, cannot be used. Thus, for most demanding conditions, 80Ni–Fe (e.g., 80% Ni, 15% Fe, 5% Mo), widely known by its commercial name of Mumetal [1], but also by several other names such as Permimphy [2], Permalloy, or Supermalloy, is usually used. However, for volumetrically large structures, due to cost implications, the shielding can sometimes also be provided by the magnetically inferior but significantly less expensive Supra 50 (around 50% Ni, 50% Fe) [3].

In some applications, extremely complex shapes are required, and they cannot be easily manufactured from a single piece of input material in the form of a sheet (Fig. 1). Some techniques, such as metal spinning or deep drawing [4], can be used in many simpler cases, but inevitably there are some shapes that require welding a larger shape from several smaller pieces, as shown in Fig. 1. Various cutting techniques can be employed, with laser beam becoming more popular in the recent years, especially due to the advances made in CNC machining (CNC — computer numerical control).

Fig. 1. An example of a magnetic shield with a relatively complex shape, manufactured with the use of laser beam cutting, bending, and welding.

It is well known that the magnetic properties of Ni-based alloys are very sensitive to chemical composition and thermal treatment conditions, both during original manufacturing and further

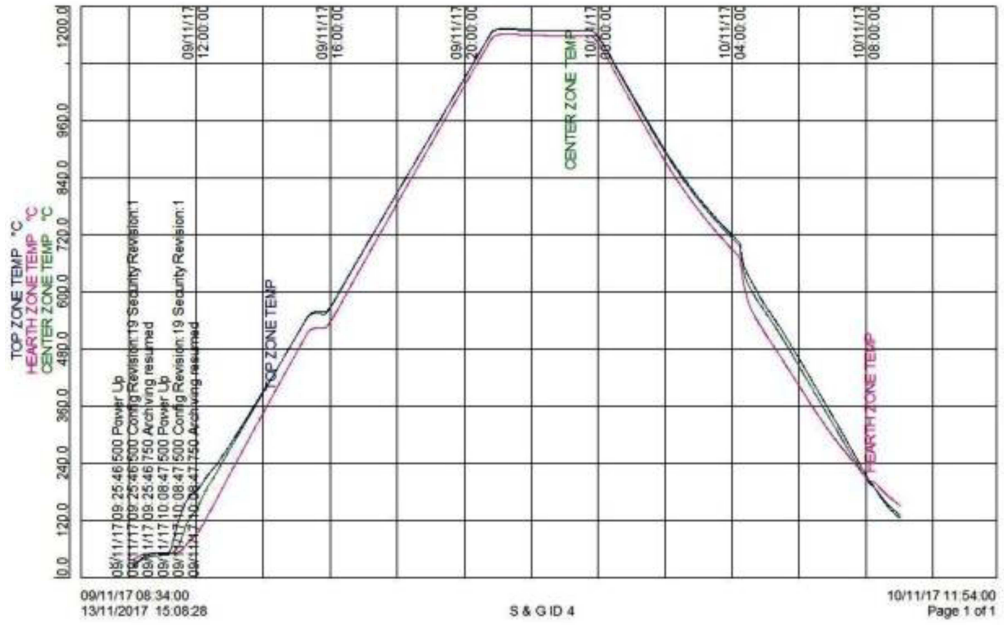

Fig. 2. Typical annealing profile used for thermal treatment of an 80Ni–Fe alloy, as dictated by [7] and performed by Magnetic Shields Ltd. [4].

mechanical and thermal processing [5, 6]. Therefore, a welding process of Mumetal and Supra 50 shields is typically carried out without adding any foreign material (also referred to as "filler") to the welded joint, and with a protective atmosphere of an appropriate inert gas, so that oxidisation and other chemical reactions are reduced to a minimum [4].

However, any type of welding is an extremely violent operation, from several view-points, the major ones being the extreme temperatures, by definition exceeding the melting point of the alloy and the comprising metals, as well as the excessive mechanical stresses resulting from the rapid and unequal heating of the welded parts, and the way the heat distributes itself in the welded part during cooling. After welding, significant residual stress remains in and around the welded joint, as well as in the remainder of the welded component.

For this reason, after welding, the magnetic shielding material must be thermally treated in order to restore, or at least improve, the magnetic properties through partial re-crystallisation and reduction of mechanical stresses. The annealing process is typically recommended by the manufacturer of a given alloy [7]. In order to control any damaging chemical processes (such as oxidisation or carburisation), annealing is carried out under a controlled atmosphere, such as vacuum (more difficult) or dry hydrogen (used more widely in industry). A typical thermal profile of annealing is shown in Fig. 2, where the applied temperature is 1100°C, held for 3 h, with controlled ramping up and ramping down at a rate of 110°C per hour, as required by [7]. Similar standard heat treatment procedures are utilised for magnetic properties damaged by mechanical stresses induced by milling, drilling, bending, deep drawing, riveting, and similar purely mechanical operations, as well as cutting by means of a guillotine or a laser beam.

However, compared to an unwelded or otherwise mechanically or thermally undamaged material, the magnetic properties of welded material can be significantly degraded even after meticulous control of all the manufacturing steps. This study was carried out in order to investigate the likely level of material degradation resulting from welding and the possibility of recovering the properties by using a standard annealing procedure in dry hydrogen, widely applied in the industry.

2. Experimental methodology and measured results

The samples were prepared as "toroidal" rings cut out from a 1.5 mm thick sheet. The outer and inner diameters were OD = 60 mm and ID = 40 mm, respectively. The cutting was carried out using a CO_2 laser. The toroidal shapes were chosen so that the magnetic measurements could be carried out by following the procedure defined in the standard IEC 60404-6 [8].

The same choice of sample types was repeated for two nickel-based high-permeability magnetic alloys, i.e., 80Ni–Fe Mumetal nd 50Ni–Fe Supra 50. Three types of rings were produced and analysed, as shown in Fig. 3. Initially, i.e., before further processing for the experiments (as described below), all three groups had the same nominal dimensions.

TABLE I

Average weight of samples, calculated from batches of 5 samples.

	uncut	2 cuts	4 cuts
80Ni–Fe Mumetal	20.48 g / 100.00 %	20.40 g / 99.61 %	20.18 g / 98.54 %
50Ni–Fe Supra 50	19.28 g / 100.00 %	19.12 g / 99.17 %	18.90 g / 98.08 %

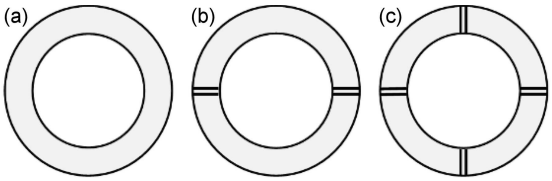

Fig. 3. Sample geometry: (a) uncut, (b) 2 cuts, (c) 4 cuts.

The first group was the "uncut" samples (Fig. 3a), which served as the reference or the "control group". These were subjected to the same type of processing, i.e., laser cutting and annealing, in the same manner as all the other samples (obviously, apart from cutting and welding). Therefore, any changes resulting from processing but not caused directly by cutting and welding should be similar in all the investigated samples.

In the second group, the ring samples were cut in half (2 cuts, Fig. 3b) and re-welded back into a full ring (Fig. 4). The aim was to restore the sample affected by cutting and welding back to a toroid-like shape so that magnetic measurements by means of [8] could be carried out with the same level of precision. It should be noted that since the shapes and sizes were nominally the same, the magnetic measurements could be relied upon in the sense of relative comparisons, where the absolute accuracy of the measurement system was less relevant [9], and thus negligible in this study.

In the third group, the ring samples were cut into four parts (4 cuts, Fig. 3c) and then also re-welded back into a full ring, for the same reason as in the second group. The same welding process was used for this group, and therefore the images in Fig. 4 are representative for the group in Fig. 3b and Fig. 3c. For the cutting operation, the parts of the rings were not completely separated, but very small "bridges" (< 0.5 mm) were left near the outer perimeter, as can be seen in Fig. 4a. These bridges were used to ensure that the re-welding operation can be carried out with improved precision in the shape of the final ring. These bridges were completely melted and "overwelded", as evident in Fig. 4b.

The hypothesis for this study was that by comparing the degradation of permeability for each group, it should be possible to extract information about the degradation of just the welded zone by applying an appropriate mathematical model for the magnetic circuit.

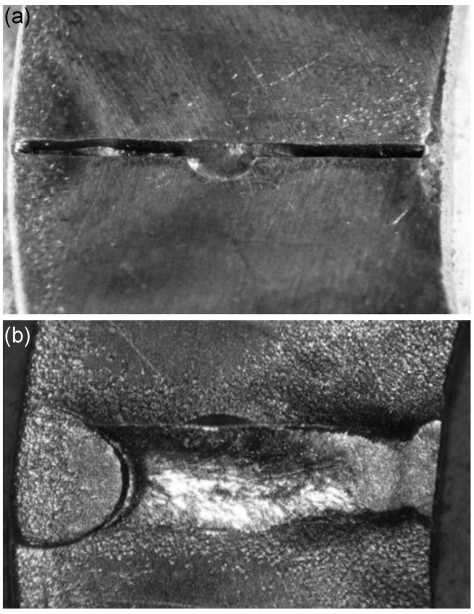

Fig. 4. Close-up view: (a) cut welded from just one side (the half-weld is underneath in this picture, shown here for illustration only), (b) cut re-welded into a full joint (by welding operation completed on both sides of the ring).

Each group contained 5 samples (15 in total), and therefore each data point was averaged from 5 measurements, which allowed reducing "noise" in the obtained quantities due to inherent variation in the welding procedure, which was carried out manually.

The magnetic properties of the samples were measured with peak flux density B varied in steps from 5 mT to 0.5 T, at 50 Hz and 400 Hz, under conditions of controlled waveshape of sinusoidal flux density (as per [8]), obtained with digital feedback [9, 10]. During the magnetic measurements, the peak flux density was controlled to within 0.2%, and the deviation from the "form factor" (ratio of root mean square to average) to within 0.5%, which is more stringent than required by the IEC 60404-6 standard [8]. The measurements were performed with 10 turns of primary winding and 10 turns of secondary winding, each of which was uniformly distributed around the circumference of the toroid sample.

The cutting resulted in some material loss, so that the cut samples were slightly lighter than the reference ones (Table I). This was caused by the fact

that no foreign filler material was used during the welding. The 80Ni–Fe samples were heavier because of a specific density of 8700 kg/m^3, as compared to 8200 kg/m^3 for 50Ni–Fe. The difference in specific density is caused by the differences in alloy content.

Each sample was weighted, and the average from the whole batch was used as a value for each sample for the magnetic measurements. This approach was taken because there was a certain amount of variation in dimensions due to mechanical tolerances, and it was not practical to provide precise information about each individual sample, especially after welding, which caused some additional mechanical distortions.

Typical permeability curves measured during this study are shown in Fig. 5a for 80Ni–Fe and in Fig. 5b for 50Ni–Fe. These graphs show only the averaged curves, for brevity, as the main information is presented later in the paper. The curves are qualitatively very similar, so only two sets are shown for brevity.

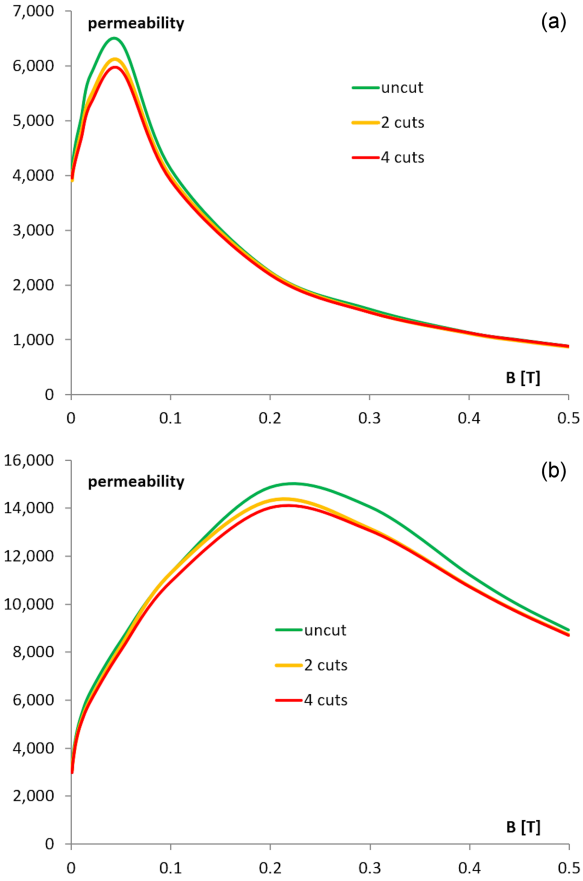

Fig. 5. Global permeability of: (a) Mumetal at 400 Hz, (b) Supra 50 at 50 Hz.

3. Mathematical model and analysis

Small degradation of the global permeability curves (a few percent) is visible with increasing number of cuts, as evident in Fig. 5a, b. However, the changes were rather small, and they were subjected to a significant amount of scattering due to variations in the industrial process of sample preparation, such as welded joint width or material loss due to cutting, as well as the finite precision of B control. For this reason, the variations were too big to be analysed directly, and further averaging had to be employed, as explained below.

A reasonable assumption was made that 4 cuts were affecting twice as much material as 2 cuts, but a significant amount of metal in a ring could be assumed to be largely unaffected because it was not directly welded. Therefore, an appropriate equivalent mathematical reluctance model was constructed to take these assumptions into account.

As can be seen in Fig. 4b, the directly affected zone for each welded joint was much wider, visually estimated to be around 2.5 mm on average. This comprised material that has been melted (visible change in shape). Obviously, more material must have been impacted thermally in the immediate vicinity of the weld [9]. However, for the non-melted metal, any potential degradation was likely to be significantly smaller than it was in the case of the melted joint. For this reason, it was assumed for analysis that the width of all the welded joints was 2.5 mm, and this value was used in calculations, as described below.

The analysis was based on a simplified reluctance model, as shown in Fig. 6. The same approach was used for the 2-cut model and the 4-cut model,

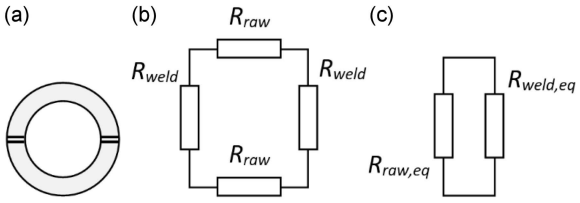

Fig. 6. Simplified reluctance model for a sample with 2 cuts: (a) sample with 2 welds, (b) equivalent model with 2 raw and 2 welded parts, (c) simplified equivalent reluctance circuit. An analogous model was used for 4 welds.

but obviously scaled accordingly by the number of welds, and thus the number of reluctance values in the ring circuit. Thus, the reluctance of each part (raw or welded) was calculated as

$$R = \frac{l}{\mu_0 \, \mu_r \, A}, \tag{1}$$

where l [m] is the magnetic path length based on average diameter, μ_0 [H/m] — permeability of free space, μ_r [H/m] — relative permeability of the material, A [m^2] — average cross section area of the sample.

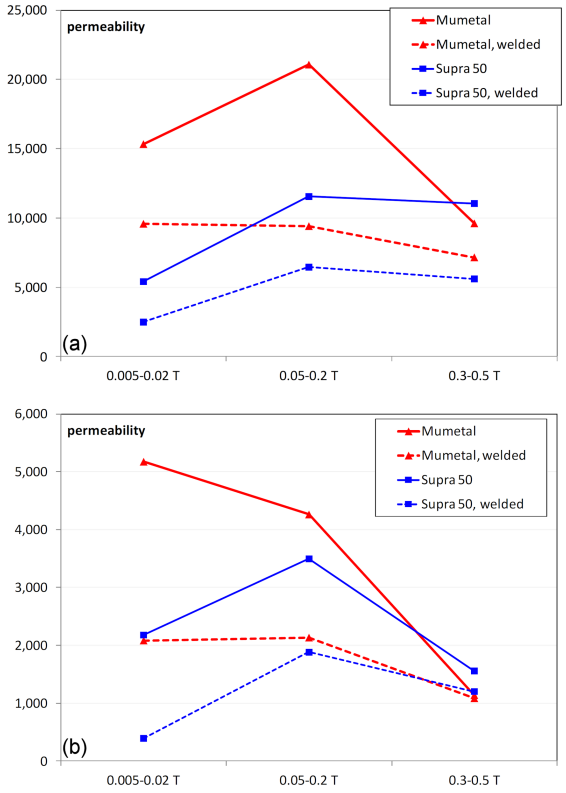

Fig. 7. Extracted relative permeability for: (a) 50 Hz, (b) 400 Hz.

The value of μ_r for the raw (not melted) material was extracted in each case by using data from the reference (uncut) samples. For the uncut samples, the average magnetic path length l [m] was calculated from the average of the outer diameter OD and the inner diameter ID, thus

$$l_{\text{raw, uncut}} = \pi \frac{\text{OD} + \text{ID}}{2}. \tag{2}$$

As mentioned above, the weld length was assessed to be 2.5 mm. For the cut samples, the length of the raw material could be calculated by subtracting the multiplicity of the welded joints from the total value calculated from (2).

The total permeability for each sample batch was measured, so the total reluctance R_{tot} was calculated directly from (1). The small weight loss of the samples (as indicated in Table I) was assumed to be insignificant in the reluctance analysis.

Hence, the equivalent reluctance of the melted material can be extracted by using the approach shown in Fig. 6b. This can be done by taking into account that for the cut samples, the magnetic path length of the raw material was proportionally shorter due to the presence of the welded joints. The percentage of the melted material in the whole volume of the sample estimated in this way was 3.2% for 2 cuts and 6.4% for 4 cuts (because twice as much material was affected in the 4-cut samples as it was for the 2-cut samples).

Therefore, taking into account the appropriate magnetic path lengths, it can be written that the equivalent reluctance $R_{\text{weld,eq}}$ [1/H] for the welded material is (see also Fig. 6c)

$$R_{\text{weld, eq}} = R_{\text{tot}} - R_{\text{raw, eq}}. \tag{3}$$

This value can then be converted back to permeability by rearranging equation (1) since all other variables are known, including the length of the welds (either 2×2.5 mm for 2 cuts or 4×2.5 mm for 4 cuts).

In order to decrease the scattering of the calculated data, the final values were averaged from the 2-cut and 4-cut calculations. This was carried out on the fairly safe assumption that the degradation of each welded joint itself was similar, regardless of the total number of cuts present in the sample. To further "smooth out" the variations, the values were averaged to represent three distinct ranges of B: low — from 5 to 20 mT, medium — from 50 mT to 0.2 T, and high — from 0.3 to 0.5 T. The global permeability curves shown in Fig. 5a, b are non-linear, but such an approach of averaging "by range" was justified because all the curves followed very similar patterns, and for the purpose of this analysis, they could be treated as "sufficiently linear" to justify such an approach. Therefore, a given percentage change within each range would be similar for that range, regardless of the actual non-linear values.

4. Combined results and analysis of magnetic degradation

The results of the analysis described above for 50 Hz are shown in Fig. 7a, and for 400 Hz in Fig. 7b. These graphs show extracted values of permeability for the raw material (unwelded, solid curves) and the welded joints (dashed curves). All the following curves show the values averaged from the models for 2-cut and 4-cut samples, so that only one value for the welded joint material is reported.

It can be seen that in all cases, the welded material exhibits visibly lower permeability. The corresponding percentage values are shown in Fig. 8a, b. These are the same data as in Fig. 7a, b, but presented as a percentage of permeability, with respect to the reference point of the raw material. Namely, for each data point in the above-mentioned figures, the percentage of permeability of the raw material is assumed to be 100%, and for each point, the permeability of the welded joints is shown as relative to 100% reference of the raw material.

At 50 Hz, the permeability of the welded material is reduced to around 45–75% of the raw material. At 400 Hz, the degradation appears to be far greater for lower amplitudes, but not very significant for the highest amplitudes. This can be explained by the fact that at 400 Hz and high excitation, the

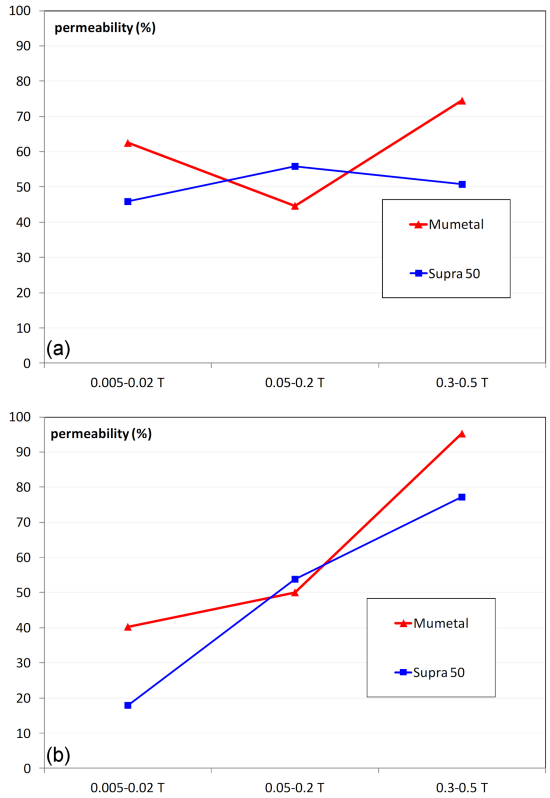

Fig. 8. Extracted percentage permeability of welded joints (raw material = 100%) at: (a) 50 Hz, (b) 400 Hz.

contribution of eddy currents to the power loss, and thus the apparent reduction in global permeability, is quite high, and the permeability is severely reduced anyway (see Fig. 5). Therefore, any reduction in permeability will be less pronounced under such conditions. This is partially dictated by the approach described in IEC 60404-6 [8], because at elevated frequencies, the permeability based on the peak of the flux density B_p and the peak of the magnetic field strength H_p becomes ill-defined [9]. Therefore, an analysis based on such values can be significantly affected, especially for thicker samples, as was the case in this study.

The relatively large sheet thickness (1.5 mm) of the samples was chosen consciously, because this enabled more repeatable results from manual welding, and it was directly relevant to a specific industrial application (Fig. 1). Otherwise, it would not be possible to ensure that the local thickness of the welded joint was reasonably similar to the unwelded parts. And as evident in Fig. 4, even in this case, the thickness of each joint was affected, so it is clear that these effects would be exacerbated for thinner samples.

Nevertheless, the impact at low excitation amplitudes at 400 Hz appears to be very strong. It is possible that this behaviour is linked to the skin effect. At 50 Hz, the skin depth for Mumetal would be around 0.3 mm, so that only a part of the cross section area would be conducting the flux, but the changes in permeability with amplitude are around a factor of 2 (i.e., 50% reduction in Fig. 8a). However, at 400 Hz, the permeability changes with amplitude by a factor of around 6 (see also Fig. 5a), and thus greater non-linearity of skin effect can be expected through the depth of the lamination.

An alternative explanation could be that at 400 Hz, the population and mobility of domain walls are affected differently. The number of domains tends to increase at higher frequencies, as it is also known for other materials [11]. If the crystallographic composition of the material is changed due to welding (which is inevitable after such a violent thermo-mechanical operation as welding), then the behaviour of domain walls can be affected. Crystallographic studies to confirm such effects were not conducted in this research, as it was beyond the scope of this study.

5. Conclusions

Welding of 80Ni–Fe Mumetal and 50Ni–Fe Supra 50 reduces the relative permeability of the melted material in a measurable way. For 1.5 mm thick material at 400 Hz and low excitation (below 20 mT), the reduction could be such that the welded joint permeability is reduced by as much as 60% for Mumetal and 80% for Supra 50, compared to the raw, non-welded material. At medium excitation between 50 and 200 mT for 50 Hz and 400 Hz, the reduction is around 45–75% of the raw material value.

However, if the welded joints constitute a relatively small volume of the total shield, then the overall permeability of the magnetic shield as a whole (rather than the isolated permeability of the welded joint) is impacted in a relatively minor way. This is because a "short" joint will have relatively low reluctance due to its limited length, in the sense of magnetic path length.

References

[1] Magnetic Shield Corp., MuMETAL® Technical Data (accessed Aug. 2025).

[2] Aperam, Permimphy, Cold Rolled Strip, 2025 (accessed Aug. 2025).

[3] Aperam, Supra 50, Supra 50 SP Cold Rolled Strip, 2025 (accessed Aug. 2025).

[4] Magnetic Shields Limited, Manufacturing (accessed Aug. 2025).

[5] R.M. Bozorth, *Ferromagnetism*, IEEE Press, 2003.

[6] R. Hilzinger, W. Rodewald, *Magnetic Materials, Fundamentals, Products, Properties, Applications*, Wiley 2013.

[7] Aperam, Softe Magnetic Heat Treatment, FeNi50, FeNI80, 2020 (accessed Aug. 2025).

[8] IEC 60404-6:2018, "Magnetic materials — Part 6: Methods of measurement of the magnetic properties of magnetically soft metallic and powder materials at frequencies in the range 20 Hz to 100 kHz by the use of ring specimens", 2021.

[9] S. Zureks, *Characterisation of Soft Magnetic Materials Under Rotational Magnetisation*, Taylor & Francis / CRC Press, 2017.

[10] S. Zurek, *Prz. Elektrotech.* **2017**, 16 (2017).

[11] Y. Sasaki, *IEEE Trans. Magn.* **16**, 569 (1980).